A discrete S=1 model for electron localization in biferrocenium salts. II. Application to Mossbauer data

1993 J. Phys.: Condens. Matter 5 5179

(http://iopscience.iop.org/0953-8984/5/29/013)

J. Phys.: Condens. Matter 5 (1993) 5179–5188. Printed in the UK

A discrete S=1 model for electron localization in biferrocenium salts: II. Application to Mössbauer data

K Boukheddaden†‡, J Linares†‡, S Galam§‖ and F Varret†‡

†Département de Recherches Physiques, Tour 22, 4 place Jussieu, 75252 Paris Cédex 05, France

§Groupe de Physique des Solides, Tour 23, 2 place Jussieu, 75251 Paris Cédex 05, France

Received 1 February 1993

Abstract. The thermal dependence of Mössbauer spectra of various biferrocenium derivative salts is obtained using the cooperative spin-1 model presented previously. Both second- and first-order delocalized–localized transitions are reproduced accurately. An apparent thermal equilibrium between localized and delocalized states found in several cases is discussed within the framework of the model.

1. Introduction

In the first paper of this series [1], a Blume–Emery–Griffith (BEG) Hamiltonian was found to provide a qualitative explanation for the various thermal behaviours of electronic localization exhibited by mixed-valence biferrocenium derivative salts in the solid state.

The atomic structure of biferrocenium is sketched in figure 1. The BEG Hamiltonian uses a fictitious spin $S = 1$, associated with a three-level system which results from the discretization of the configurational diagram of the biferrocenium cation (figure 2). Such a particular, triple-well-shaped, diagram is obtained through an extension of the standard Piepho–Schatz–Krausz (PKS) model [2] to account for the degeneracy of the highest occupied molecular orbital (HOMO) [3–5]. With a two-fold HOMO, the diagram is made up of four curves, i.e. two pairs of 'standard' PKS curves. It is discretized in terms of a three-level system which mimics the different properties of the lowest curve of each PKS pair.

In this second paper, we apply this spin-1 model to the quadrupole splitting data available for biferrocenium derivative salts. It is worth recalling that localization in biferrocenium salts exhibits a large variety of properties at the Mössbauer timescale which is of order $\sim 10^{-8}$ s (for a recent review, see [6]). There exist trapped or averaged states at all temperatures, onset of localized–delocalized transitions of first or second order, and coexistence of localized and delocalized components with progressive conversion, which suggests a thermal equilibrium process. So far, only the second-order transition has been successfully modelled. The observed dependence on the X substituents (figure 1), the counteranion and the packing, gives evidence for the importance of both the intra- and intermolecular aspects of the problem, which are represented as well in the $S = 1$ Ising-like cooperative model of [1].

‡ Laboratoire associé au CNRS (UA no 71) et à l'Université Pierre et Marie Curie.

‖ Laboratoire associé au CNRS (UA no 17) et aux Universités Paris VII et Pierre et Marie Curie.

0953-8984/93/295179+10$07.50

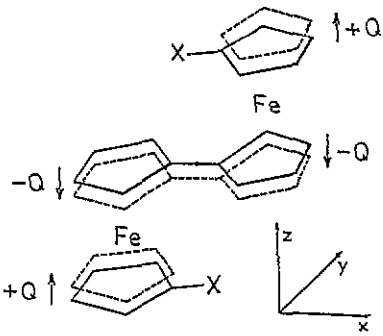

Figure 1. Schematic view of the biferrocenium cation (X = H) and derivatives (X ≠ H), with the asymmetric distortion Q_-.

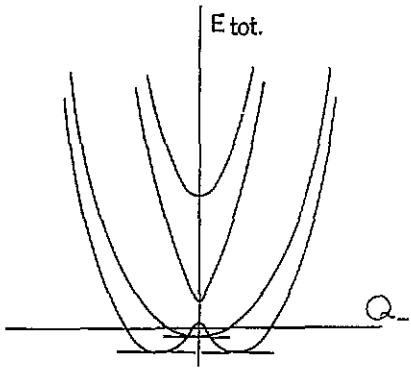

Figure 2. Configurational diagrams, i.e. adiabatic energy curves plotted agaisnt Q_- in the extended PKS case, computed for the case of the biferrocenium cation (after [1]). Horizontal bars denote the three levels considered in the present mode. An external asymmetric potential lifts the degeneracy of the doublet.

The paper is organized as follows. Section 2 contains a presentation of the Blume–Emery–Griffiths model of [1]. Analysis of the experimental data is presented in section 3. Section 4 is devoted to a discussion of the results and the last section presents our conclusions.

2. Ising-like model with $S = 1$

The three-level system which models the molecule (figure 2) is described by a fictitious spin $S = 1$. The pair of levels in the double well is associated with $S_z = \pm 1$; the single level in the single well with $S_z = 0$ and a two-fold degeneracy. This additional degeneracy has been introduced to account for the different vibrational properties of the double and single wells in the Born–Oppenheimer approach. $S_z = 0, \pm 1$ can be considered respectively as 'delocalized' and 'localized' states. In the solid state, interacting $S = 1$ systems are described by the Blume–Emery–Griffiths (BEG) Hamiltonian [7],

$$\hat{\mathcal{H}} = -\sum_{\langle i,j \rangle} J_{ij}\hat{\sigma}_i\hat{\sigma}_j - \sum_{\langle i,j \rangle} K_{ij}\hat{\sigma}_i^2\hat{\sigma}_j^2 + \sum_i \Delta_i\hat{\sigma}_i^2 \tag{1}$$

where $\hat{\sigma}_i$ is the projection of the ith spin on the quantization axis. J and K are interaction terms due to the intermolecular crystal field. The eigenstates of $\hat{\mathcal{H}}$ are $\sigma_k = 0, \pm 1$ (note that the last sign (+) in equation (2) of [1] was missing).

All contributions to equation (1) are relevant to the mixed valence problem. We have: $+\Delta_i\hat{\sigma}_i^2$ expresses the energy difference between the singlet and doublet of the isolated ith molecule. It is a single-spin anisotropy term originating from the intramolecular low-symmetry ligand field. $-J_{ij}\hat{\sigma}_i\hat{\sigma}_j$ is a contribution to the pair energy which lifts the degeneracy of the doublet by spontaneous symmetry breaking. $-K_{ij}\hat{\sigma}_i^2\hat{\sigma}_j^2$ is a second contribution to the pair energy, which does not lift the degeneracy of the doublet.

The mean-field approximation leads to the one-site Hamiltonian,

$$\hat{\mathcal{H}}_{\mathrm{mf}} = \tfrac{1}{2}(Jm^2 + Kq^2) + \Delta\hat{\sigma}^2 - Jm\hat{\sigma} - Kq\hat{\sigma}^2 \tag{2}$$

where the first-order parameter $m = \langle\hat{\sigma}\rangle$ denotes the degree of localization with $m = \pm 1$ for trapped valence, i.e. charge ordered state, and $m = 0$ for a delocalized state, either statically (population of $\sigma = 0$ state only), or statistically (equipopulation of $\sigma = \pm 1$ states, with eventually fast electron transfer). The second-order parameter $q = \langle\hat{\sigma}^2\rangle$ accounts for the relative population of the localized states. The strength and the number of intermolecular interactions are represented by J and K.

Eigenstates of $\hat{\mathcal{H}}_{mf}$ are $\sigma = +1, 0, -1$, with eigenvalues $E_0 = \frac{1}{2}(Jm^2 + Kq^2)$ and $E_{\pm 1} = E_0 + \Delta \mp Jm - Kq$. Deriving the partition function Z and free energy $F = -k_B T \ln(Z)$ gives

$$Z = [2 + 2\exp[\beta(Kq - \Delta)]\cosh(\beta Jm)]\exp[-\tfrac{1}{2}\beta(Jm^2 + Kq^2)] \tag{3}$$

and

$$F = \tfrac{1}{2}(Jm^2 + Kq^2) - k_B T \ln[2 + 2\exp[\beta(Kq - \Delta)]\cosh(\beta Jm)] \tag{4}$$

where $\beta = 1/k_B T$. Minimization of F with respect to m and q leads to the coupled system

$$m = \frac{2\exp[\beta(Kq - \Delta)]\sinh(\beta Jm)}{2 + 2\exp[\beta(Kq - \Delta)]\cosh(\beta Jm)} \tag{5}$$

and

$$q = \frac{2\exp[\beta(Kq - \Delta)]\cosh(\beta Jm)}{2 + 2\exp[\beta(Kq - \Delta)]\cosh(\beta Jm)}. \tag{6}$$

When this system of self-consistent equations has several solutions (symmetrical and non-symmetrical), the most thermodynamically stable is selected. Typical variations of the order parameters are schematized in figure 3, some of them ($J > 0$) leading to an order–disorder transition of first or second order.

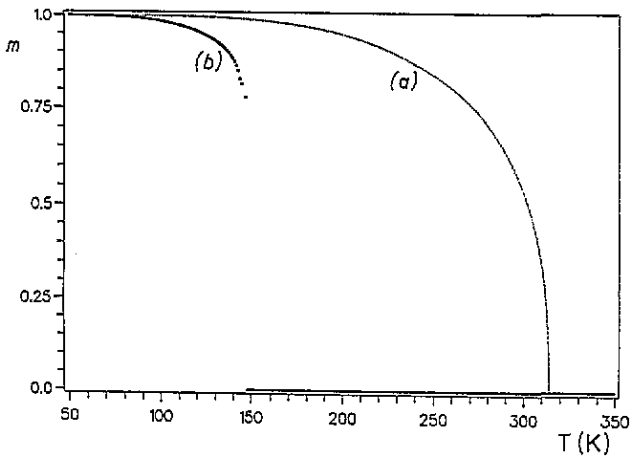

Figure 3. Typical thermal variations of the order parameter m with order–disorder transitions: (*a*) second-order, obtained with $J = K = 500$ K, $\Delta = 150$ K. (*b*) first-order, with $J = K = \Delta = 500$ K.

The quadrupole interaction is expressed through the thermal average of the electric field gradient (EFG) components of the three states. The 'average' state $\sigma = 0$ contributes as the average of $\sigma = \pm 1$ states. The following correspondence (with A, B denoting the moieties of the mixed-valence cation) is assumed, with

$\langle\sigma\rangle = -1$: Fe(A) = Fe(II); Fe(B) = Fe(III)

$\langle\sigma\rangle = +1$: Fe(A) = Fe(III); Fe(B) = Fe(II)

$\langle\sigma\rangle = 0$: Fe(A) = Fe(B) = Fe(av).

The EFG components are expressed as

$$V_{ij}^{A,B} = [V_{ij}^{II,III}\exp(-\beta E_{-1}) + V_{ij}^{III,II}\exp(-\beta E_{+1}) + (V_{ij}^{II} + V_{ij}^{III})\exp(-\beta E_0)]/Z. \tag{7}$$

The quadrupole splitting value is derived from the principal components of the EFG, giving

$$QS = [\tfrac{2}{3}(V_{XX}^2 + V_{YY}^2 + V_{ZZ}^2)]^{1/2}. \tag{8}$$

To minimize the number of free parameters fitting quadrupole data, the following assumptions, based on molecular orbital calculations [5] are made. The Fe^{II} tensor has axial symmetry around the molecular z axis. The Fe^{III} tensor has a non-zero asymmetry parameter and its main axis lies in the molecular xy plane. Then the EFG can be put in terms of only three free parameters: two quadrupole splittings, QS^{II}, QS^{III}, which are easily deduced from the low-temperature spectra, and one asymmetry parameter η^{III}, whose value can be derived by trial and error from the value of the quadrupole splitting above the ordering temperature.

3. Analysis of the experimental data

Three well-documented cases where a localization transition has been observed are now considered.

3.1. Diethyl biferrocenium triiodide

We have investigated a well-crystallized sample of diethyl biferrocenium triiodide (sample kindly provided by Dr S Nakashima), with special care in the vicinity of the critical temperature ~ 280 K detected by earlier studies [8]. Selected Mössbauer spectra obtained using transmission integral techniques are shown in figure 4. On the Mössbauer timescale, the low-temperature state is valence-trapped, with spectra made of two doublets typical for Fe^{II} and Fe^{III} moieties; when temperature is increased, the Mössbauer lines of the two moieties move towards each other and at 283 K collapse into a single doublet typical for the valence-averaged state. At all temperatures the lines remain narrow, and indicate that the electron transfer rate always remains far from the Mössbauer frequency ($\sim 10^8$ Hz). Due to the observation of a valence-trapped state at the IR timescale at room temperature, it was concluded [8] that the transfer rate remained *higher* than the Mössbauer frequency. This conclusion supports the calculation of the quadrupole splitting in terms of a thermal average (as we have done in the previous section).

The experimental Mössbauer data are summarized in table 1. Rather good agreement with the computed variation is found (figure 5) with a Δ value sufficiently large (and negative) to make negligible the effect of the $\sigma = 0$ state. Fitted parameters are

$J = 280$ K

$QS(Fe^{II}) = 1.92$ mm s^{-1} $\qquad QS(Fe^{III}) = 0.52$ mm s^{-1} $\qquad \eta(Fe^{III}) \simeq 0.2.$

It is worth mentioning that in such a case the model reduces to an Ising spin-$\frac{1}{2}$ model (i.e. to a two-level system).

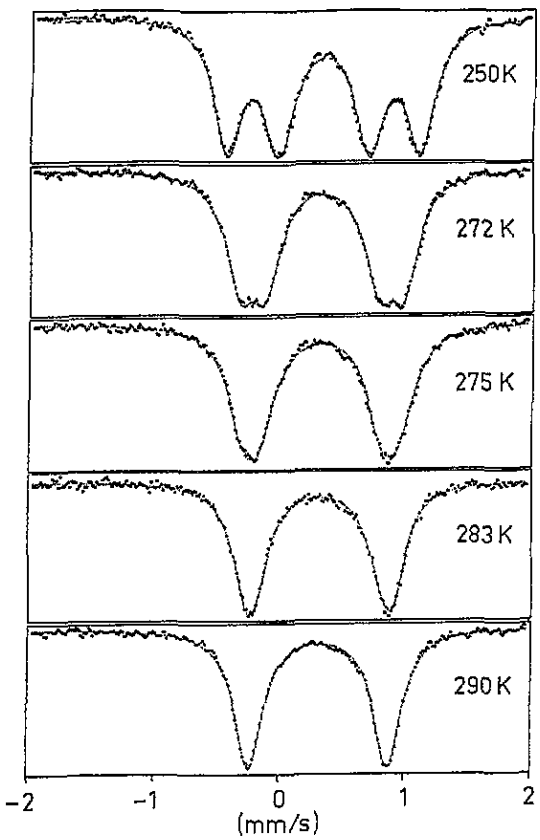

Figure 4. Selected Mössbauer spectra of diethyl biferrocenium triiodide.

Table 1. ^{57}Fe Mössbauer least-squares fitting parameters for diethyl biferrocenium triiodide (in mm s^{-1}).

T(K)	δ_1^*	Γ_1	QS_1	δ_2^*	Γ_2	QS_2
260	0.453(2)	0.286(4)	0.814(3)	0.458(2)	0.266(4)	1.494(3)
265	0.452(2)	0.296(4)	0.857(3)	0.457(2)	0.280(6)	1.442(3)
268	0.448(2)	0.302(4)	0.891(4)	0.452(1)	0.278(6)	1.415(4)
270	0.448(2)	0.308(6)	0.936(6)	0.453(2)	0.300(8)	1.364(6)
273	0.448(2)	0.306(8)	0.947(8)	0.450(2)	0.296(8)	1.320(8)
275	0.446(2)	0.316(8)	1.017(1)	0.449(3)	0.27(1)	1.325(1)
276	0.449(2)	0.324(6)	1.043(1)	0.452(3)	0.24(1)	1.314(1)
278	0.448(2)	0.312(3)	1.06(2)	0.444(2)	0.23(1)	1.28(2)
280	0.442(4)	0.312(4)	1.09(2)	0.447(3)	0.22(2)	1.25(3)
282	0.446(2)	0.310(4)	1.11(2)	0.444(5)	0.19(6)	1.27(4)
283	0.442(2)	0.310(3)	1.133(2)			
285	0.445(2)	0.300(2)	1.128(2)			
290	0.440(2)	0.290(2)	1.136(2)			
295	0.438(2)	0.306(3)	1.128(2)			
300	0.434(2)	0.298(3)	1.128(2)			

* The isomer shifts δ are reported with respect to metallic iron at room temperature.

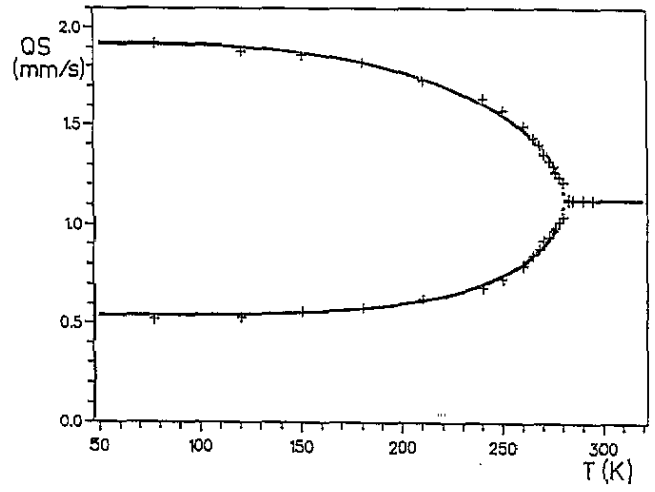

Figure 5. Measured quadrupole splittings of diethyl biferrocenium triiodide, and best fit using the present model (values given in section 3.1).

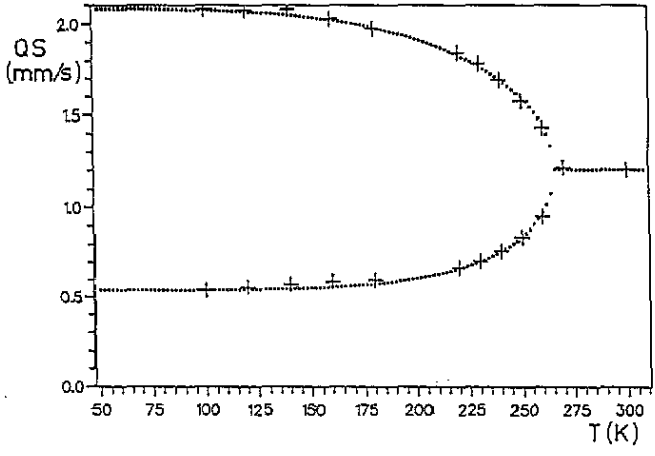

Figure 6. Measured quadrupole splittings of diiodo biferrocenium hexafluoroantimonate (after [9]), and best fit using the present model (values given in section 3.2).

3.2. Diiodo biferrocenium hexafluoroantimonate

The structure of the diiodo biferrocenium cation is shown in figure 1 (with X = I). Quadrupole splitting data have been reported by Webb *et al* [9]. Similar to the previous casee, a fusion-type behaviour of the Mössbauer spectra associated with a very small peak of the specific heat is reported near $T_{OD} \sim 270$ K. The thermal dependence of quadrupole splittings is not well reproduced by a spin-$\frac{1}{2}$ model. A better fit (figure 6) is obtained with the following parameters:

$$J = 417 \text{ K} \qquad K = 121 \text{ K} \qquad \Delta = -73 \text{ K}$$
$$\text{QS}(\text{Fe}^{\text{II}}) = 2.08 \text{ mm s}^{-1} \qquad \text{QS}(\text{Fe}^{\text{III}}) = 0.54 \text{ mm s}^{-1} \qquad \eta(\text{Fe}^{\text{III}}) \simeq 0.0.$$

It is interesting to compare the thermal variation of the order parameters for these two cases of 'fusion-type' behaviour. It is shown in figure 7. The excited $\sigma = 0$ state appears to make the $m(T)$ curve shape more square-like.

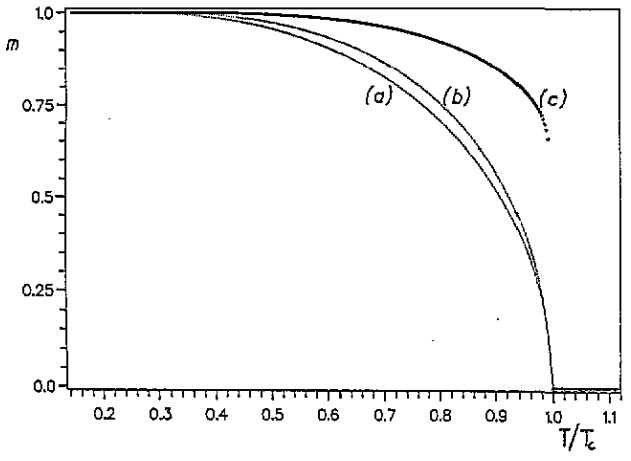

Figure 7. Computed thermal variations of the order parameter m for diethyl biferrocenium triiodide (*a*), diiodo biferrocenium hexafluoroantimonate (*b*) and biferrocenium triiodide (*c*), in reduced temperature scale.

3.3. Biferrocenium triiodide

Biferrocenium triiodide is a textbook example extensively studied [10, 11] which exhibits a sharp variation of the Mössbauer spectra in a relatively narrow temperature range. In this 'critical' range, the shape of the specific heat anomaly and the Mössbauer spectra are spectacularly dependent upon the preparation conditions of the sample (crystal defects and stresses). Available data in this critical range are reported in figure 8. They can be reasonably reproduced with several sets of parameters; for instance,

$$758\ \text{K} \leqslant J \leqslant 774\ \text{K} \qquad K = 750\ \text{K} \qquad \Delta = 500\ \text{K}$$

$$QS(Fe^{II}) = 2.11\ \text{mm s}^{-1} \qquad QS(Fe^{III}) = 0.35\ \text{mm s}^{-1} \qquad \eta(Fe^{III}) \simeq 0.2.$$

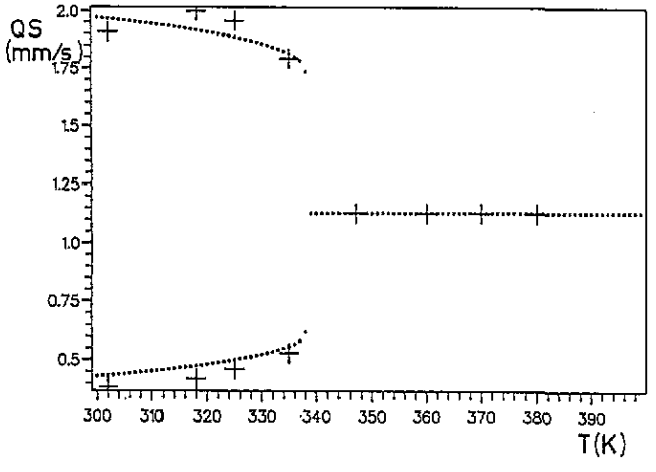

Figure 8. Measured quadrupole splittings of biferrocenium triiodide (after [11]), and best fit using the present model (values given in section 3.3).

4. Discussion

Using the present discrete level model we have successfully reproduced the transitions exhibited by mixed-valence salts. The above three cases illustrate the influence of low-energy excited states associated with the quasi-degeneracy of the HOMO: on decreasing $E(x^2-y^2)-E(xy)=-\Delta$, the shape of the thermal variation of the order parameter, shown in figure 7, progressively deviates from a pure Ising $S=\frac{1}{2}$ behaviour to a more squared shape, eventually leading to a first-order behaviour for Δ larger than a threshold value. Although such a discrete model reproduces the transitions observed so far adequately, we found it useful to consider a full vibronic treatment, *a priori* more suited to the biferrocenium salts, because the validity of the Born–Oppenheimer approach is obviously questionable in the case of a $d_{x^2-y^2}$ HOMO. Such an elaborate model, involving a two-fold HOMO, is under study. We have already reported the results of a preliminary 'cooperative PKS' model involving a non-degenerate HOMO [12].

At the present stage of analysis of the intriguing properties of biferrocenium and biferrocenium-like salts, there remains to be understood the coexistence of localized and delocalized components in the Mössbauer spectra of *biferrocenium diiodo bromide* [13] and dibutyl biferrocenium triiodide [14], over surprisingly large temperature ranges: 150–300 K and 240–300 K (at least), respectively.

The trivial explanation in terms of a distribution of ordering temperatures, due to a poor crystalline quality of the samples, can stand for a temperature range of some tens of K, as evidenced by the various samples of biferrocenium triiodide investigated in [13, 14]; it seems to be ruled out for both cases reported here. Then the problem must be put in terms of a *thermal equilibrium between localized and delocalized states, with conversion rates which are lower than the Mössbauer frequency.* This is analogous, both theoretically and experimentally, to the spin conversion, which is better known (see [15] for a general review of spin-crossover complexes), and explained in terms of a thermal competition between different electronuclear states characterized by different spins, energies and degeneracies [16]. Such a competition between spin states has been successfully described by a two-level Ising-like model [17] in close analogy with the present model.

Then the relative area n_{loc} of the localized component of the Mössbauer spectrum can be considered as a measurement of the order parameter q. This, however, in the present model, is true only in the charge-ordered state ($m \neq 0$). Indeed, in the disordered state ($m = 0$) the molecules behave as isolated molecules in symmetrical surroundings. Since computed electron transfer rates must be *in any case* [4] higher than the Mössbauer measuring frequency, then the observed ratio n_{loc} should drop to zero. Typical computed variations $m(T)$, $q(T)$ and $n_{loc}(T)$ are shown in figure 9. It is important to note that any variation of the m parameter should be reflected in a variation of the quadrupole splittings of the localized components. Quadrupole splittings of the 'localized components', calculated through equation (3) restricted to $\sigma = \mp 1$ states, are also plotted in figure 9.

Experimental data are definitively at variance from the expectations summarized in figure 9 with the following two remarks.

(i) The shape of $n_{loc}(T)$, reported in figure 10, basically differs from the typical expected shape, and

(ii) the QS values of the localized components are practically temperature independent.

In addition, there is no obvious reason for conversion rates, between delocalized and localized states of unsubstituted biferrocenium salts, to be low when the counteranion is I_2Br^- and high for almost all other counteranions (the experimental case of PF_6^- [13] remains unclear).

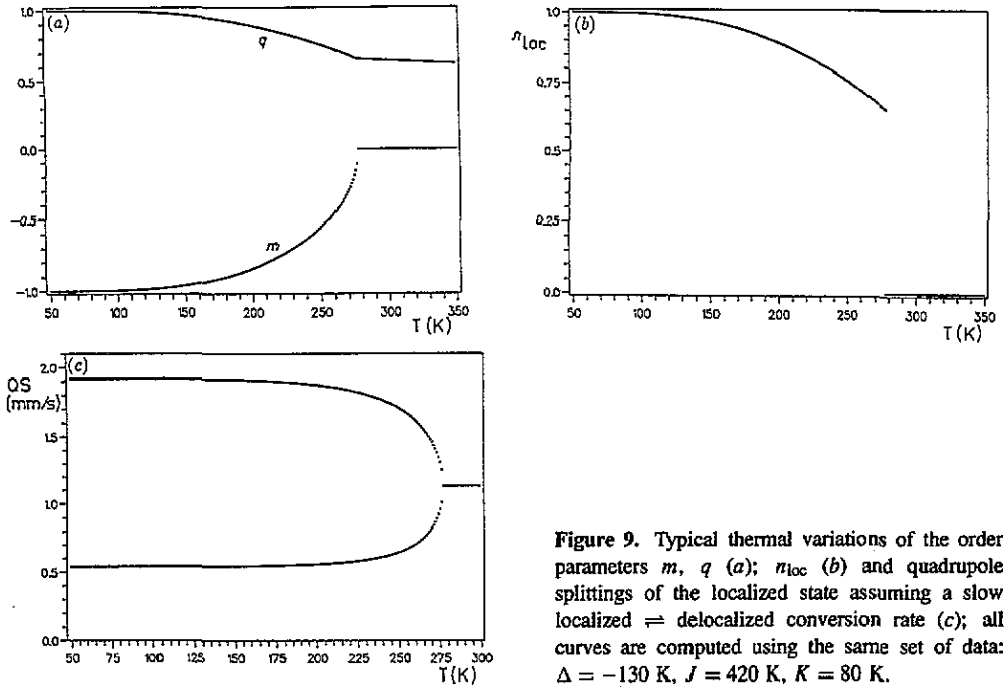

Figure 9. Typical thermal variations of the order parameters m, q (a); n_{loc} (b) and quadrupole splittings of the localized state assuming a slow localized $\rightleftharpoons$ delocalized conversion rate (c); all curves are computed using the same set of data: $\Delta = -130$ K, $J = 420$ K, $K = 80$ K.

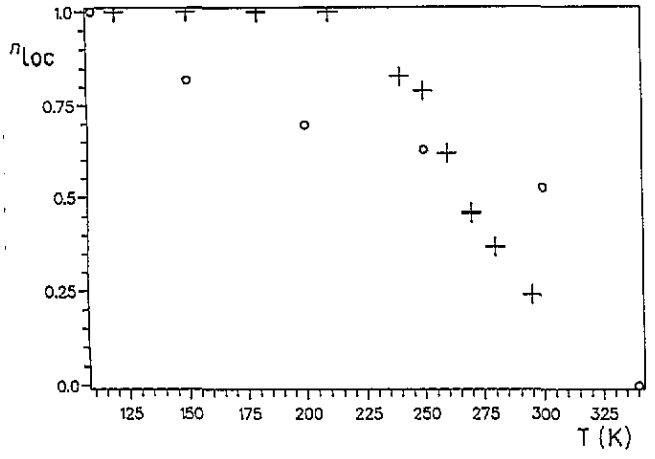

Figure 10. Experimental variation of $n_{loc}(T)$, for biferrocenium diiodobromide (○) and dibutyl biferrocenium triodide (+), after [13, 14] respectively.

We think that both the above discrepancies, as well the above unanswered question, might be solved in terms of short-range ordering. This phenomenon of course has been discarded in the mean-field treatment. In a system such as the present one, which possesses two order parameters, short-range order is a complex problem which involves both charge-ordered and disordered 'domains' (in the dynamical sense), as usual order–disorder systems do, but also delocalized domains. One easily imagines that intermolecular interactions, which are known to slow down the electron transfer rates of 'localized' molecules: $(\sigma = -1) \rightleftharpoons (\sigma = +1)$, can also slow down the localized–delocalized conversion rates: $(\sigma = \pm 1) \rightleftharpoons (\sigma = 0)$. Both theoretical work and accurate experimental data in the vicinity of the ordering temperature are needed to solve this exciting problem.

5. Conclusion

Most of the Mössbauer data concerning biferrocenium salts can be reproduced by using the Ising-like model with $S = 1$, which provides a (mean-field) thermodynamic description of the electronic localization. It is clear that a complete understanding of the mixed valence problem must also describe the short-range order, i.e. the dynamics of the electron transfer and of the conversion between the localized and delocalized states.

Acknowledgment

We thank Phan-Xuan-Huy for graphical assistance.

References

[1] Boukheddaden K, Linares J, Galam S, Varret F 1993 *J. Phys.: Condens. Matter* **5** 1–9
[2] Piepho S B, Krausz E R and Schatz P N 1978 *J. Am. Chem. Soc.* **100** 2996–3005
[3] Varret F, Rabah H, Guillin J and Talham D 1991 *Mixed Valence Systems: Applications in Chemistry, Physics and Biology* ed K Prassides (Dordrecht: Kluwer) pp 359–64
[4] Boukheddaden K, Linares J, Bousseksou A, Nasser J, Rabah H and Varret F 1993 *Chem. Phys.* **170** 147–56
[5] Rabah H 1990 *PhD Thesis* Université du Mans
[6] Hendrickson D N 1991 *Mixed Valence Systems: Applications in Chemistry, Physics and Biology* ed K Prassides (Dordrecht: Kluwer) pp 67–90
[7] Blume M, Emery V J and Griffiths R B 1971 *Phys. Rev.* A **4** 1071–7
[8] Ijima S, Saida R, Motoyamal and Sano H 1981 *Bull. Chem. Soc. Japan* **54** 1375–9
Nakashima S and Sano H 1989 *Chem. Lett.* 1075–8
Nakashima S , Nishimori A, Masuda Y, Sano H and Sorai M 1991 *J. Phys. Chem. Solids* **52** 1169–80
[9] Webb R J, Hagen P M, Wittebort R T, SoraïM and Hendrickson D N 1992 *Inorg. Chem.* **31** 1791–801
[10] Sorai M, Nishimori A, Hendrickson D N, Dong T Y, and Cohn M J 1987 *J. Am. Chem. Soc.* **109** 4266–75
[11] Cohn M J, Hendrickson D N, Geib S J and Rheingold A L 1985 *J. Chem. Soc., Chem. Commun.* 1095
[12] Boukheddaden K, Linares J and Varret F 1993 *Chem. Phys.* at press; 1993 *Phys. Rev.* B at press
[13] Dong T Y, Kambara T and Hendrickson D N 1986 *J. Am. Chem. Soc.* **108** 4423–32
[14] Dong T Y, Hendrickson D N, Iwai K, Cohn M J, Rheingold A L, Sano H, Motoyama I and Nakashima S 1985 *J. Am. Chem. Soc.* **107** 7996
[15] Gütlich P 1981 *Struct. Bonding* **44** 83
Rao C N R 1985 *Int. Rev. Phys. Chem.* **4** 19
[16] Wajnsflasz J and Pick R 1971 *J. Physique Coll.* **32** C1 91
Kambara T, Hendrickson D N, Dong T Y and Cohn M J 1987 *J. Chem. Phys.* **86** 2362–74
[17] Bousseksou A, Nasser J, Linares J, Boukheddaden K and Varret F 1992 *J. Physique I France* **2** 1381–403; 1992 *Proc. European Conf. on Molecular Electronics ECME '92 (Padova)* to be published